Materials & Design 185 (2020) 108223

Contents lists available at ScienceDirect

Materials & Design

journal homepage: www.elsevier.com/locate/matdes

Bioactivity of catalase loaded into vaterite $CaCO_3$ crystals via adsorption and co-synthesis

Natalia A. Feoktistova [a], Anna S. Vikulina [b, c, *], Nadezhda G. Balabushevich [a], Andre G. Skirtach [d], Dmitry Volodkin [a, c]

[a] Department of Chemistry, Lomonosov Moscow State University, Leninskiye Gory 1-3, Moscow, 119991, Russia
[b] Fraunhofer Institute for Cell Therapy and Immunology, Branch Bioanalytics and Bioprocesses, Am Mühlenberg 13, 14476, Potsdam-Golm, Germany
[c] School of Science and Technology, Nottingham Trent University, Clifton Lane, Nottingham, NG11 8NS, UK
[d] Department of Biotechnology, University of Ghent, Coupure Links 653, 9000 Ghent, Belgium

HIGHLIGHTS

- Catalase partially loses its enzymatic activity while pre- or post-loaded into vaterite crystals.
- Activity reduction is due to both protein exposure to alkaline medium during loading and Ca^{2+}-induced protein aggregation.
- Amount of catalase loaded into the crystals is pH-independent while catalase activity strongly depends on pH.
- Protein aggregation significantly governs protein release performance.

GRAPHICAL ABSTRACT

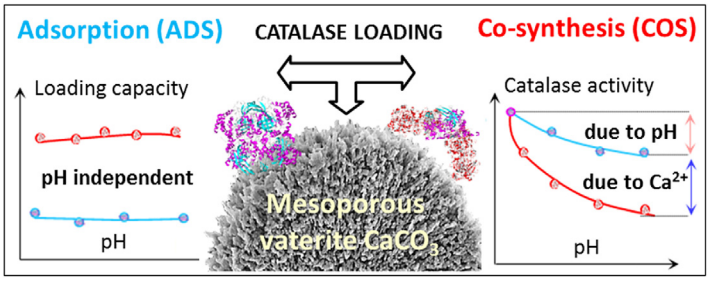

ARTICLE INFO

Article history:
Received 30 April 2019
Received in revised form
18 September 2019
Accepted 19 September 2019
Available online 5 October 2019

Keywords:
Encapsulation
Calcium carbonate
Circular dichroism
Co-synthesis
Mesoporous

ABSTRACT

Protein therapy gained a reputation of the most direct and safe approach for treating various diseases, yet biodegradation and loss of bioactivity of fragile therapeutic proteins limit their wide medical use. Recently, a new hard templating technology using decomposable mesoporous vaterite $CaCO_3$ crystals became extremely popular strategy for formulation of protein nano(micro)-vectors. This study deciphers how protein bioactivity depends on protein loading/release for this technology utilizing catalase as a promising antioxidant therapeutic agent. Catalase has been loaded into $CaCO_3$ using two approaches: i) passive - via adsorption (ADS) into pre-formed crystals and ii) active - via co-synthesis (COS) in the pH range 8–10. Crystal morphology, protein secondary structure and enzymatic bioactivity, and protein retention upon washing are assessed. The activity reduction (~70% for COS and ~20% for ADS) is caused by both protein exposure to an alkaline medium and protein aggregation induced by Ca^{2+}. The aggregation significantly governs protein release kinetics. Catalase loading into the crystals is pH-independent and van der Waals interactions dominate over the electrostatics, while catalase activity strongly depends on pH. This study implicates the prime role of loading/release mechanism in the preservation of protein bioactivity and guide for the control over the retention of protein bioactivity.

1. Introduction

Proteins have been reported as effective therapeutic agents due

* Corresponding author. Fraunhofer Institute for Cell Therapy and Immunology, Branch Bioanalytics and Bioprocesses, Am Mühlenberg 13, 14476, Potsdam-Golm, Germany.
E-mail address: Anna.vikulina@izi-bb.fraunhofer.de (A.S. Vikulina).

https://doi.org/10.1016/j.matdes.2019.108223

to their high bioactivity, selectivity, and reduced side effects [1–3]. There is a strong demand in encapsulation of proteins into nano- and micro-particulate systems, because this allows one to enhance the protein stability, protect proteins against enzymatic degradation in order to increase their life-time, tune protein release profile, and achieve targeted protein delivery. Protein encapsulation that allows the preservation of protein bioactivity and control over the size and physical-chemical properties of the carrier remains a challenge. Therefore, scientific attention has turned to mild encapsulation approaches which avoid typical problems of traditional methods, e.g. organic solvents; additives such as surfactants; shear forces and heat; creating additional interfaces; etc.

Modern strategies for protein/peptide delivery include their derivatization, prodrug approach, the use of mucoadhesive polymers and formulation vehicle, wherein emulsions, nanoparticles, microspheres and liposomes are the major classes of the carriers used for proteins and peptides delivery. Although all of them have obvious advantages, remaining challenges include the loss of protein activity, physiochemical instability, high product development costs, and others which are described elsewhere [4]. Among others, different mesoporous inorganic particles are of especial interest and promise [5,6] because their pore diameters match the typical size range for biomacromolecules (from a few nm to tens of nm) that facilitates the encapsulation. A variety of mesoporous materials also has enormous loading capacity (because of their large pore volume), no need to chemically modify the therapeutic molecules, and the options for control via external stimuli [7,8], theranostic [9] and multidrug loading [10]. Unfortunately, the majority of them require harsh preparation or elimination (when used as sacrificial templates) conditions.

Porous vaterite $CaCO_3$ crystals have shown high promise as inorganic templates for mild encapsulation [11,12]. $CaCO_3$ has attracted attention because it is one of the most abundant natural biominerals [13] that is non-toxic and approved by U.S. Food and Drug Administration (FDA). The vaterite crystals are made of nanocrystallines binding to each other and forming channel-like pores of typical dimensions of a few tens of nm (mesoporous structure). It is rather easy to synthesize vaterite $CaCO_3$ microcrystals at supersaturated conditions [11] or by using supercritical CO_2 process [14]. Some recent reports indicate a trend for preparation of nano-sized vaterite crystals that may open new perspectives to employ the crystals for intracellular delivery [15–20]. The crystal porosity can be adjusted even with no additives by varying the preparation temperature that affects the nanocrystalline growth through the Ostwald ripening [21–23]. Also, the crystal morphology can be tuned at the supersaturated conditions [24,25].

In recent years, vaterite crystals have been successfully employed as drug vehicles or as sacrificial templates to assemble polymer-based carriers such as multilayer capsules or beads. The multilayer capsules are highly attractive carriers for encapsulation through $CaCO_3$-based templating giving an option to adjust the efficiency and loading capacity [12,26], and a release rate of encapsulated compounds by varying the properties of the multilayers [7,27–30]. Not only large compounds like proteins [31–35] and biopolymers [36,37] but also small drugs of different nature have been encapsulated using the crystals [15,38–40]. Other examples include encapsulation of small and large bioactive molecules, e.g. polyethylene glycol [41,42], poly(N-isopropylacrylamide) [43]. The applications of the crystals are mainly focused on drug delivery [44–49]. High affinity of $CaCO_3$ crystals to mucin [37,50] (a major component of human mucus) opens perspectives for the use of $CaCO_3$ crystals for mucosal drug delivery, e.g. ocular [51] or intravesical delivery [52]. Alternative applications have also been reported, for instance, in personal care, cosmetics, food industry, sensors, scaffold materials, etc. [8,53–58]. Despite the fact that the crystals have been employed for encapsulation of different biomolecules, the primary focus in regard with encapsulation in $CaCO_3$ has been on encapsulation of proteins, because of mild decomposition conditions of the crystals (slightly acidic pH, EDTA, or citric acid), simple synthesis procedure, biocompatibility, low costs, and the pore size in the range of protein size allowing to effectively host proteins and potentially release them in a sustained manner.

Proteins can be effectively loaded into the crystals using passive loading through physical adsorption into performed crystals (ADS) or active loading through co-synthesis (COS) when the protein molecules are added to the salts used for the crystal growth (e.g. $CaCl_2$ and Na_2CO_3) [35,59,60]. Despite ADS can result in inhomogeneous loading due to steric limitations for protein molecules to diffuse through the crystal pores, COS is not only very efficient in terms of the loading content but also can provide a homogeneous protein distribution [59].

Although there is a strong evidence of the importance of protein loading into the crystals, the retention of protein bioactivity after encapsulation into the crystals is not well reported. The $CaCO_3$ crystals hydrolyse in water that induces an increase of pH to alkaline pH of about 10. The pH 10 may not be attractive in regard with biological relevance, because this alkaline pH significantly differs from the physiological one (pH 7.4). This may affect bioactivity of proteins in the crystal suspension for either passive or active encapsulation. This study aims to evaluate the effect of $CaCO_3$-based encapsulation through passive and active loading on the protein bioactivity. Catalase is used for this purpose as a well-characterized model protein [61,62]. Our previous paper [60] have already given some insights into the mechanism of catalase loading into the crystals and revealed the important role of catalase aggregation induced by the presence of Ca^{2+} ions during COS. Bearing this in mind, we now addressed the question of the retention of catalase specific activity and in this view also considered the effect of pH on both loading efficiency and retention of enzyme activity. Encapsulation in the range of pH 8–10 has been performed using a buffer to keep pH constant during the loading. Protein secondary structure and bioactivity have been assessed after dissolution of the protein-containing crystals in EDTA.

2. Experimental section

2.1. Materials

$CaCl_2{}^*2H_2O$ and Na_2CO_3 anhydrous from Sigma-Aldrich; catalase from bovine liver (3809 units/mg solid) from Sigma; glycine buffer (0.05 M, pH 9.0), phosphate buffer (0.05 M, pH 7.0), TRIS buffer (0.05 M, pH 7.0, 8.0, 9.0), hydrogen peroxide and ethylenediaminetetraacetic acid (EDTA) from Sigma-Aldrich. NaCl from Panreac Quimica San. Water used in all experiments was prepared via a Millipore Milli-Q purification system and had a resistivity higher than 18.2 MΩ cm.

2.2. Preparation of $CaCO_3$ crystals

Porous crystals were prepared by a rapid mixing of equal volumes of $CaCl_2$ and Na_2CO_3 aqueous solutions at 22 °C. Briefly, $CaCl_2$ (3 mL, 1 M) was added to H_2O (9 mL) at constant stirring, then Na_2CO_3 (3 mL, 1 M) was rapidly added to the solution at 22 °C. After vigorous agitation with a magnetic stirrer (40 s) and incubation (15 min), the precipitate was separated by centrifugation (1000 g), thoroughly washed two times with pure water and dried at 80 °C giving the crystals with the size of 4–5 μm.

2.3. Protein loading into $CaCO_3$ crystals by ADS

Catalase solutions (1.5 mL, 1–2 mg mL^{-1}) in glycine (0.05 M) or TRIS buffer with appropriate pH was added to dry $CaCO_3$ crystals (60 mg) and incubated during 30 min followed by centrifugation for 5 min at 10000 g and twice repeated rinsing. All supernatants were collected and examined to determine the protein concentration using UV spectroscopy (280 nm).

2.4. Protein loading into $CaCO_3$ crystals by COS

$CaCl_2$ (0.2 mL, 1 M) was added to catalase (0.6 mL, final concentrations during COS 1.0–4.0 mg mL^{-1}) dissolved in glycine (0.05 M) or TRIS buffer at constant stirring, then Na_2CO_3 (0.2 mL, 1 M) was rapidly added to the solution at 22 °C. Final pH in the mixture was measured and used as the pH of crystal growth during COS. After vigorous agitation with a magnetic stirrer (40 s) and incubation (15 min), the precipitate was separated by centrifugation (1000 g), thoroughly washed two times with corresponding buffer and all supernatants were collected and examined to determine the protein concentration using UV spectroscopy (280 nm). Adsorption capacity (q_e) was estimated as the amount of loaded protein under equilibrium conditions and was calculated as the loss in protein amount in supernatant (mg) divided to the mass of $CaCO_3$ (g).

2.5. Protein biological activity

Specific activity of catalase was measured by monitoring the rate of hydrogen peroxide decomposition. Catalase (0.005–0.010 mg mL^{-1}) dissolved in phosphate buffer (0.1 M, pH 7.0) and aqueous solution of hydrogen peroxide (0.100 mL of 0.196 M) has been added to 0.9 mL of catalase (0.005–0.010 mg mL^{-1}) dissolved in phosphate buffer (0.1 M, pH 7.0). Decrease in absorbance was registered at 240 nm. To measure the retention of catalase activity in the crystals, suspension of catalase-loaded $CaCO_3$ (2 mg in 100 mL of phosphate buffer, 0.1 M, pH 7.0) has been dissolved in 100 mL of EDTA (0.2 M) followed by the addition of H_2O_2 (0.100 mL of 0.196 M) and monitoring of absorbance at 240 nm. Retention of catalase activity was calculated as the ratio between the activities of the enzyme recovered after crystals dissolution in EDTA (0.2 M) and the catalase of equal concentration in phosphate buffer (pH 7.0).

2.6. Dynamic light scattering (DLS) and ζ-potential measurement

Hydrodynamic diameters were determined by DLS using a Zetasizer Nano ZS (Malvern Instruments Limited, Worcestershire, UK). Values were reported as intensity, volume, and number weighted particle size distributions (PSD). The surface charges were determined using ζ-potential measurements (and evaluated using the Smoluchowski function) for $CaCO_3$ microparticles suspended in Milli-Q water (1–20 mg mL^{-1}). ζ-potential of catalase at different pH was measured using 0.2 mg mL^{-1} solution of the catalase in 0.05 M TRIS buffer.

2.7. Circular dichroism (CD)

CD spectra were recorded by Jasco J-815 CD Spectrometer. The Jasco J-815 CD Spectrometer (wavelength range 163–900 nm) is a hybrid instrument consisting of a variable wavelength polarimeter and absorption spectrophotometer. It is designed to allow secondary structure determination by circular dichroism; specifically measuring the left-and right-handed circularly polarized light of optically active molecules. It is equipped with a computer-controlled Peltier device (3–90 °C) and a two-syringe titrator to assess thermal/chemical stabilities of proteins/polypeptides or to monitor ligand binding and is controlled by Jasco's Spectra Manager software. The secondary structure of the catalase has been determined based on CD spectra correlated with X-ray diffraction data for bovine liver catalase (1TGU) from Protein Data Bank using Protein Secondary Structure Analysis Tools (CDNN).

2.8. Scanning electron microscopy (SEM)

Field emission SEM images were recorded using a Gemini LEO 1550 electron microscope at an accelerating voltage of 3 kV. Samples were prepared by dropping the crystal suspension on a glass slide, dried within 1 h at 90 °C followed by conductive coating with gold palladium (5 nm).

2.9. Brunauer, Emmett, and Teller (BET) analysis

Surface area and the porosity of the crystals have been measured by N_2 adsorption–desorption analysis using a QUADRASORB SI-MP (Quantachrome Instruments, USA) at 77.3 K. Prior to measurements, the samples were degassed at 150 °C for 20 h by BET analysis using the Barret–Joyner–Halenda (BJH) model has been used for the surface area and porosity analysis.

2.10. Statistical analysis

Statistical analysis was performed by paired Student's *t*-test using Medcalc Statistical software. The statistical significance of differences was set at $p < 0.05$.

3. Results and discussion

3.1. Effect of preparation pH on passive and active protein loading into $CaCO_3$ crystals

Passive (through ADS into pre-formed crystals) and active (COS through adding the protein during the crystal synthesis) loading approaches have been used here to encapsulate catalase into vaterite $CaCO_3$ crystals (Fig. 1).

Our recent work showed that the mechanism of catalase loading by COS involves aggregation of the protein by $CaCl_2$ during the COS process that results in inclusion of protein aggregates into the crystals during the growth [60]. The size of the formed aggregates is in the range of tens of nm (50 ± 8 nm in the presence of 0.2 M $CaCl_2$), which allows to compactly fill the pores of the crystals and therefore to load an enormous amount of the protein of up to 20 w/w %. However, in that earlier study the effect of preparation pH on crystal structure, loading capacity and retention of catalase activity have not been investigated. These issues are addressed in this study.

The catalase has been loaded by means of both COS and ADS at different pH values, e.g. pH 8.0, 9.0 and 10.0 using the TRIS buffer. Since in the previous works the loading of catalase into the $CaCO_3$ crystals by COS and ADS has been studied mainly at pH 9.0 in glycine buffer [59,63]. First, we have investigated if the nature of the buffer can play a role in affecting the protein loading into the crystals. Fig. S1 shows the dependence of the catalase content in the crystals on the catalase concentrations used for the loading by COS in glycine and TRIS buffers of the same pH, i.e. pH 9.0. No difference clearly proves that there is no effect of the chemical composition of the buffers. In this work, we have further used the TRIS buffer because it has a wide range of pH while keeping the high buffer capacity.

It is of worth to note that on the timescale of the experiments (i.e. a few hours) catalase-$CaCO_3$ hybrids were stable but underwent recrystallization into thermodynamically more favorable calcite during longer-term storage in aqueous medium with both

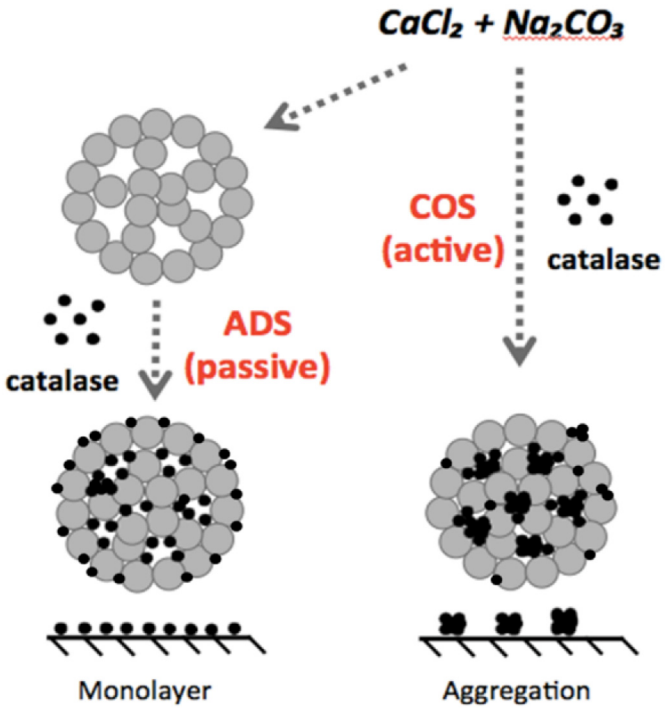

Fig. 1. Schematics of catalase loading into $CaCO_3$ crystals through passive (ADS) and active (COS) loadings.

neutral and alkaline pH. Acidic environment results in the rapid dissolution of $CaCO_3$ crystals and disintegration of catalase-$CaCO_3$ particles.

Fig. 2 compares the amount of catalase in the $CaCO_3$ crystals as a function of the preparation pH for ADS and COS. Surprisingly, the adsorption is pH independent for both loading methods and the loaded amount for COS is about twice higher than that for ADS.

One has to note that the maximum loading capacity is higher for COS and is not reached at the conditions of this experiment (Fig. 2a). The concentration dependence of the amount of catalase loaded into vaterite crystals by COS and loading efficiency for different pH values are shown in Figs. 2b and S2, respectively.

Although a slight trend of decreasing of adsorption capacity with the increase of pH is observed for higher initial concentrations of catalase, the loaded amount remains almost unchanged and the loading of catalase into $CaCO_3$ crystals by means of ADS and COS may be assumed to be pH independent. The explanation of these interesting phenomena is provided in the following section.

3.2. Electrostatic attraction between $CaCO_3$ and catalase

It is known that $CaCO_3$ crystals possess rather low surface and have low positive or negative ζ-potential (depending on preparation conditions) within the ten of mV [63,64]. The results of ζ-potential measurements of vaterite $CaCO_3$ crystals fabricated in water as well as the catalase dissolved in TRIS buffer at different pH are shown in Fig. 3. Catalase has pI 5.4 and is negatively charged at all pH values in the range 8–10.

It is also important to note that ζ-potential of vaterite $CaCO_3$ crystals does not strongly depend on preparation pH and typically varies in the range from +11 to +15 mV [64]. In other words, catalase ζ-potential depends on pH while vaterite ζ-potential is almost pH-independent. Further, we have evaluated the significance of the change in catalase ζ-potential at different pH on the attraction of the catalase to vaterite crystals.

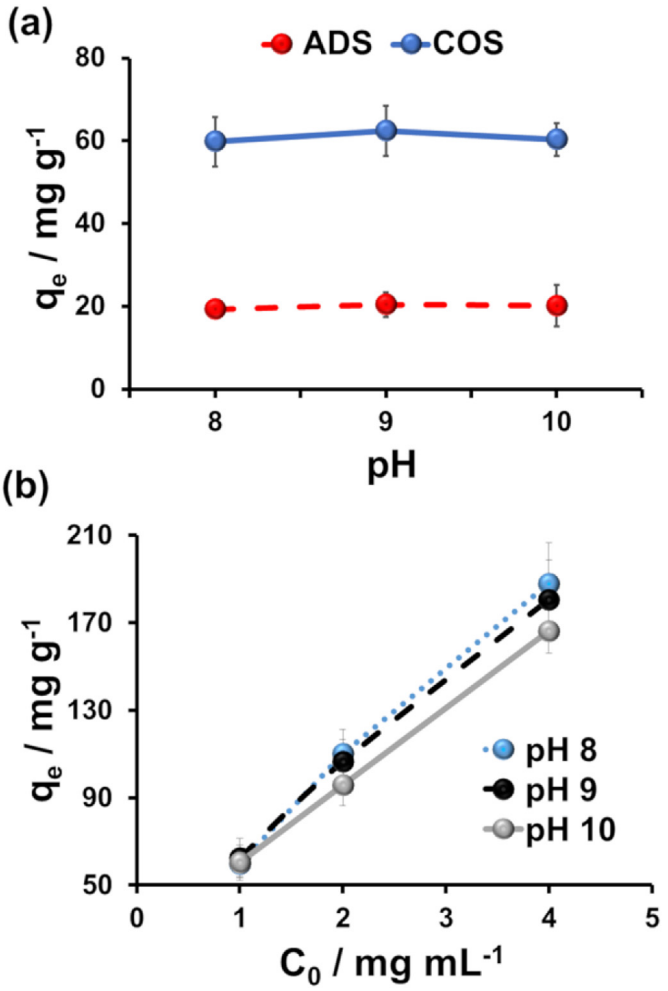

Fig. 2. (a) The amount of catalase in the $CaCO_3$ crystals (q_e) as a function of the loading pH for ADS and COS. Catalase was loaded from a 1 mg mL^{-1} stock solution. (b) The amount of catalase loaded into $CaCO_3$ crystals by COS as a function of the initial concentration of catalase stock solution at different pH.

If any specific and hydrophobic interactions are neglected, the free energy of adsorption (ΔG_{ads}) can be calculated as the superposition of the electrostatic interaction potential $\Delta u_{els}(h)$ and the van der Waals interaction potential $\Delta u_{vdW}(h)$ (Equation (1)).

$$\Delta G_{ads} = \Delta u_{els}(h) + \Delta u_{vdW}(h) \quad (1)$$

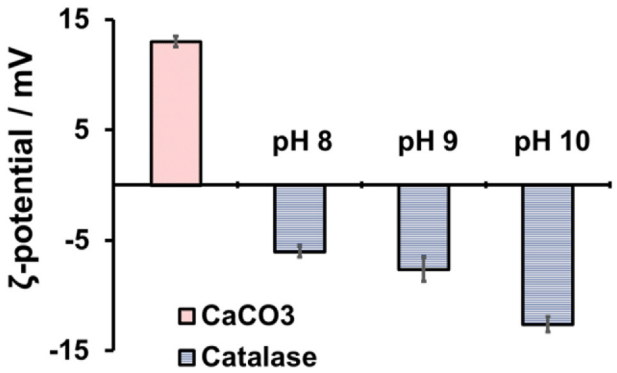

Fig. 3. ζ-potential of vaterite $CaCO_3$ crystals in water and catalase in 0.05 M TRIS buffer solution at different pH.

Here, the electrostatic potential strongly depends on the ζ-potential and therefore on pH, while van der Waals interactions are pH-independent.

First, we have assessed the van der Waals potential. The classical approach developed by Hamaker and generalized for the case of spherical particles of different size and materials has been applied (Equation (2)).

$$u_{vdW}(h) = -\frac{\sqrt{A_1 A_2}}{6}\cdot\left[\frac{2r_1r_2}{h^2+2r_1h+2r_2h} + \frac{2r_1r_2}{h^2+2r_1h+2r_2h+4r_1r_2} + \ln\left(\frac{h^2+2r_1h+2r_2h}{h^2+2r_1h+2r_2h+4r_1r_2}\right)\right] \quad (2)$$

where A_1 and A_2 – Hamaker constants of $CaCO_3$ and catalase, respectively, r_1 and r_2 – radii of $CaCO_3$ crystals and catalase molecules, respectively, h is the surface-to-surface separation distance. For the calculations, Hamaker constants of $1.44\cdot10^{-20}$ J and $1.25\cdot10^{-20}$ J have been taken for $CaCO_3$ [65] and catalase [66] in water, respectively. $r_1 = 2.5$ μm and $r_2 = 5.25$ nm have been applied.

In order to evaluate the electrostatic attraction of the catalase to vaterite crystals, the Derjaguin, Landau, Verwey and Overbeek (DLVO) theory [67] have been applied to estimate the energy of electrostatic interactions between two spherical colloids of the opposite charge – $CaCO_3$ crystal and catalase molecule. The Debye length has been calculated from Equation (3).

$$\lambda_D = \sqrt{\frac{\varepsilon\varepsilon_0 k_B T}{2N_A I e^2}} \quad (3)$$

where ε and ε_0 are the dielectric constants of the medium and vacuum, respectively, k_B is the Boltzmann constant, T is the absolute temperature, I is the ionic strength of the electrolyte, N_A is the Avogadro number, e is the charge of an electron. Debye length λ_D for 0.4 M monovalent salt solution in water at 293 K was found to be 0.48 nm. Of note, the ionic strength of 0.4 M chosen for these calculations corresponds to the final stage of $CaCO_3$ synthesis (formation of the $CaCO_3$ crystals in NaCl solution) while the first step of the mixing of the salts (prior to the crystal growth) corresponds to the ionic strength of 0.6 M. In this case, λ_D would be equal to 0.39 nm, this difference does not significantly affect further calculations.

Electrostatic potential has been assessed from Equation (4) using Hogg, Healy, and Feurstenau (HHF) equation that is derived from Derjaguin approximation for electrostatic interaction energy between two charged spheres of radii r_1 and r_2 [67].

$$u_{els}(h) = \pi\varepsilon\varepsilon_0 r^*\zeta_1\zeta_2\left\{+2\ln\left[\frac{1+e^{-h/\lambda_D}}{1-e^{-h/\lambda_D}}\right] + \frac{(\zeta_1^2+\zeta_2^2)}{\zeta_1\zeta_2}\ln\left(1-e^{-2h/\lambda_D}\right)\right\} \quad (4)$$

Here, $r^* = \frac{2r_1r_2}{r_1+r_2}$, ζ_1 and ζ_2 – ζ-potentials of $CaCO_3$ crystal and catalase molecule, respectively.

This equation expresses the interaction between the electrical double layers surrounding any two similar or dissimilar colloidal particles. It is important to note that this relationship only holds exactly for values of ζ-potential less than 25 mV and is valid for $h \ll r^*$ and $r^*/\lambda_D > 10$. All these conditions have been met in the case of the $CaCO_3$-catalase interaction.

The van der Waals and electrostatic potentials for pH 8, 9 and 10 as a function of the distance between vaterite crystal and the catalase are given in Fig. 4a indicating the dominant impact of the van der Waals potential. Summarized potential energy $u_{vdW}(h) + u_{els}(h)$ is given in Fig. 4b clearly showing that the impact of electrostatic interactions can be neglected.

Therefore, the results shown in Fig. 2 can be explained by the fact that electrostatic interactions have no influence on the catalase inclusion into the crystals in this pH range, which is related to a rather low charge of both the crystals and the catalase. At the same time, preparation pH can potentially alter the crystal morphology/structure, and this, in turn, could be the reason for pH-independent protein loading (Fig. 3). This issue is considered in the following section.

3.3. Effect of preparation pH and the presence of catalase on the $CaCO_3$ crystal structure

The crystals were synthesized in pure water at pH of about 10 due to hydrolysis of the $CaCO_3$ that gives an alkaline pH in the supernatant of the crystal water suspension. The use of the buffer gives an option to keep the pH value in the crystal suspension constant and below 10. Fig. 5a and b shows SEM images of the crystals grown in water at pH 10 and in TRIS buffer at pH 8. No significant difference in the crystal size has been observed as can be

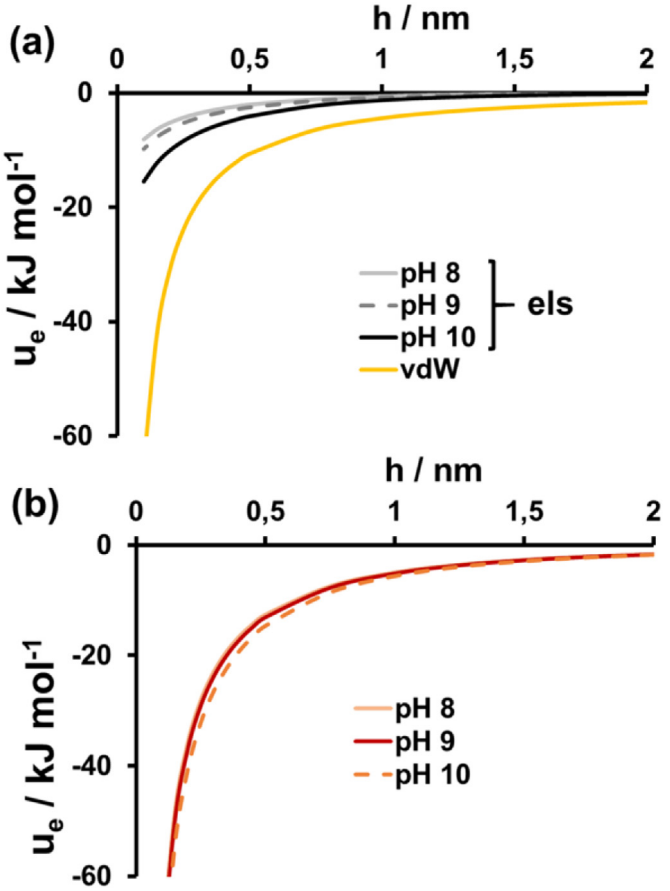

Fig. 4. (a) Electrostatic and van der Waals and (b) total attraction energy between $CaCO_3$ crystal and catalase molecule at different pH as a function of the surface-to-surface separation distance.

concluded from the reconstructed 2D surface images (Fig. 5c and d).

The crystals are made of interconnected nanocrystallines of sizes of a few tens of nm that provides a mesoporous structure of the main crystal (pore size in the range of tens of nm). The porosity of the crystals has been shown to be directly related to the roughness of the crystal surface [22]. Thus, by means of analysis of the crystal surface morphology one can make conclusions about the internal structure of the crystals. The nitrogen adsorption-desorption used for the pore structure analysis of the crystals prepared in water (pH 10) allows to calculate that the average diameter of the crystal pores is 11 ± 4 nm (BET isotherm and corresponding surface area plot are shown in Fig. S3). Since the variation of the preparation pH and the presence of TRIS buffer do not affect the crystal size and the crystal internal structure, the crystals prepared in TRIS buffer with different pH are expected to possess similar internal porosity.

In addition, the catalase itself has no to marginal effect on the internal structure of vaterite crystals as evidenced by SEM imaging of pure vaterite crystals prepared in TRIS buffer solution and crystals loaded from highly concentrated solution of the catalase ($6.67\ mg\ mL^{-1}$) by means of co-synthesis (Fig. S4). SEM imaging also proves that the presence of the catalase does not affect the polymorphism of calcium carbonate crystals (vaterite remains the dominant) although results in a slight reduction of a crystal size (data are not shown). Altogether, this means that pH independent adsorption of catalase for either ADS or COS (Fig. 2) is solely related to the protein-crystal interaction but not to the crystal internal structure.

In order to get more evidence on the role of electrostatic and van der Waals forces in catalase-vaterite interaction, catalase retention in the crystals upon the increase of the ionic strength has been investigated.

3.4. Catalase retention in the crystals: passive and active loading

Washing out the catalase from the crystals have been performed at pH 7.0 in the presence of NaCl of varied concentrations of 1, 2, and 3 M. This has been done expecting an effect of an ionic strength on both the state of the protein aggregates and on the binding of the protein molecules to the crystal surface. There is a pronounced difference in the protein retention for the methods used to load the protein into the crystals, i.e. ADS and COS. Fig. 6 demonstrates the relative absolute amount and Fig. S5 shows the absolute amount of the retaining catalase. About 38 and 3% of the protein has been washed out for ADS and COS after a few consecutive washing steps, respectively. Much slower protein release for COS compared to ADS can be explained by aggregation of the protein molecules during the COS [60].

The aggregation suppresses the protein release for the protein aggregates compared to single protein molecules that are mainly loaded into the crystals by ADS. This finding corroborates the previous report showing that bovine serum albumin loaded into the $CaCO_3$ crystals is only partly washed out [68].

With an increase of NaCl concentration in the buffer from 0 to 3 M, only little increase of the amount of released protein has been observed for both loading methods (Fig. 6). This was rather unexpected, because one can assume a more pronounced effect of the salt on the protein-crystal interaction which is primarily based on electrostatics [69]. The increased salt concentrations may induce the screening of electrostatic charges on the protein globule and

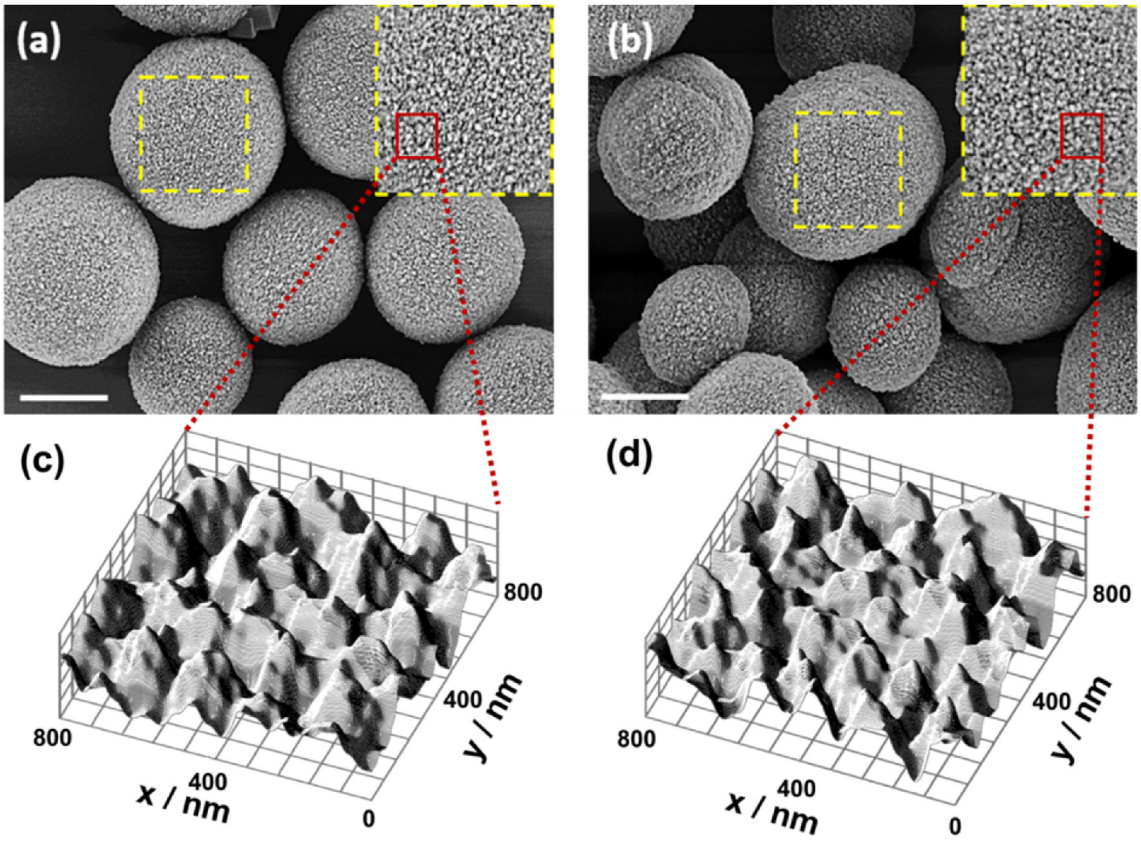

Fig. 5. SEM images of $CaCO_3$ crystals prepared (a) in water at pH 10 and (b) in TRIS buffer at pH 8. Scale bar is 2 μm. The insets are enlarged images of the interrupted yellow squares. 2D surface plots for $800 \times 800\ nm \times nm$ areas marked by red squares in (a) and (b) are shown in (c) and (d), respectively.

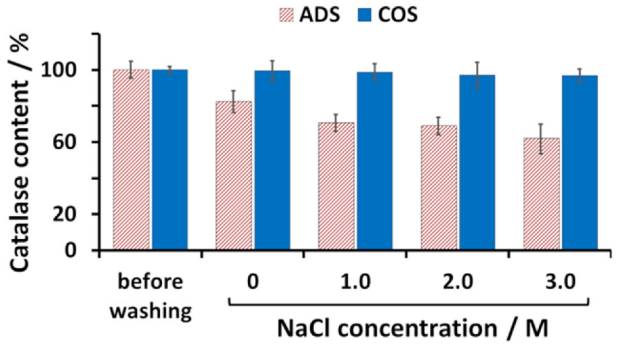

Fig. 6. The relative amount of catalase remaining in the crystals after the crystal rinsing with TRIS buffer (0.05 M, pH 7.0) in the presence of NaCl of different concentrations. The protein has been loaded in the absence of NaCl from 0.05 M TRIS buffer solution pH 7.0, with 2.0 mg mL^{-1} catalase. The initial amount of the loaded protein is taken as 100%.

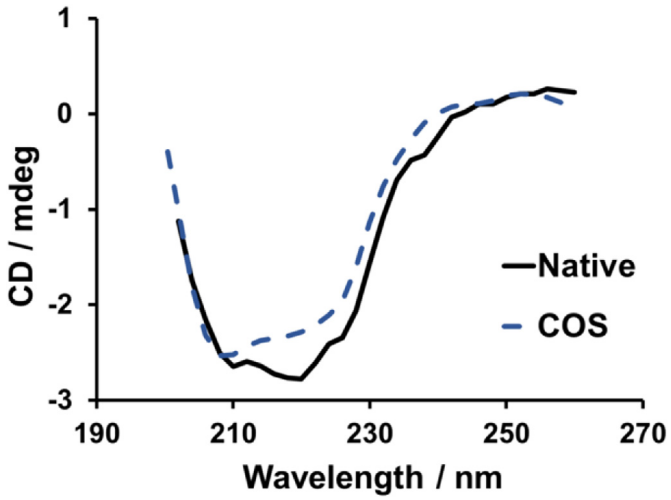

Fig. 7. Typical UV CD spectra of the native catalase in glycine buffer (pH 9.0) and catalase extracted from the $CaCO_3$ crystals by the crystal dissolution in 0.2 M EDTA followed by dialysis in glycine buffer.

thus enhancing the protein release rate. This does not occur and only a slight increase of the released protein amount has been observed at increasing salt concentrations for both loading methods (Fig. 6). At the same time, very high salt concentrations (such as 2 and 3 M) may result in stabilization of the protein aggregates into the crystals due to salting out the protein as reported for instance for chymotrypsin [70]. Such stabilization may potentially reduce the protein release rate. However, for both methods of the protein loading we did not observe neither enhancing the protein release due to the screening of the electrostatic interactions nor its suppression due to salting out and stabilization of the aggregates. This can only be explained by non-dominating contribution of the electrostatics into the catalase-crystal interaction, most probably due to low charge of the crystals. This is in a good agreement with the results shown in Fig. 2. Some examples of strong interactions of biomacromolecules with the crystals not driven by electrostatics have been reported. For instance, adsorption of almost uncharged dextrans into the prepared crystals has been found as strong as that for charged proteins [69].

3.5. Catalase structural changes during COS

CD spectroscopy has been used to estimate a change in the secondary structure of catalase loaded into the crystals followed by elimination of the crystals in EDTA and dialysis. The far-UV CD spectra of the native catalase and catalase extracted from the $CaCO_3$ crystals are shown in Fig. 7. Both spectra display a comparable shape with negative extremes in 210 and 222 nm for native catalase (which are slightly shifted for the released protein after crystal dissolution) and a zero-crossing around 201 nm. Spectra were analyzed for the contents of α-helix, α-antiparallel, β-sheet, β-turn and random coil using the Protein Secondary Structure Analysis Tools (CDNN) as presented in Table 1.

Slight decrease in α-helical content (~12% conformational change) was observed. The changes in the protein secondary structure might potentially be attributed to the exposure to EDTA during the dissolution of the $CaCO_3$ crystals. However it is known that the influence of EDTA on the protein structural changes is reversible [71] and one may expect that the effect of EDTA was neglected due to dialysis step completely removing the EDTA. In this case, the loss of α-helical content can only be associated with the protein-protein interactions and the formation of protein aggregates [72].

Although it is generally accepted that the biological activity of the enzymes is strongly dependent on conformational integrity of the enzyme molecule, it is also known that inactivation of catalase can occur without noticeable changes in its secondary structure according to the theory of flexibility at the active site [72]. Following this knowledge, biological activity of catalase loaded by COS was further investigated and described in the next section.

3.6. Catalase biological activity

It is of note that in this study we have investigated protein loading into the crystals in the view of their perspective use as sacrificial templates for polymer layer-by-layer deposition. Bearing in mind that polyelectrolyte shell might be significantly damaged upon the drying and consequent rehydration, we did not consider the recyclability of protein-loaded crystals. However, this question is important for potential employment of the crystals of $CaCO_3$ as substantive carriers for protein delivery and we hope to uncover it in our future research. Since it is known that the layer-by-layer deposition itself does not lead to the reduction of the bioactivity of pre-encapsulated proteins [59] because it is usually carried out at mild conditions, the only steps that may lead to the loss of protein activity are the entrapment of the protein and the following elimination of the $CaCO_3$ template with EDTA or other dissolution agents.

Catalase specific activity was determined by the rate of decomposition of hydrogen peroxide. Prior to the measurements, the catalase loaded into the crystals by means of COS has been extracted from the crystals by their elimination with EDTA. A study of time dependence of catalase activity in TRIS buffer solution at different pH revealed that the activity of catalase rapidly decreases in TRIS buffer within increase of pH or time (Fig. 8a). The higher is the pH, the more is the loss of the protein activity. At pH 8.0 the catalase activity does not significantly depend on time, however, at pH 10 the protein lost almost half of its activity if incubated in the buffer for 60 min compared to 15 min. The loss of enzymatic activity of catalase results from partial dissociation of catalase tetramers to inactive monomers while exposed to the alkaline pH.[71] Hence, for further analysis the enzymatic activity was measured after a fixed incubation time of 60 min and the results were presented as a percentage from the activity of the native catalase in phosphate buffer (pH 7.0) taken as 100%. The results shown in Fig. 8b clearly demonstrate that the active encapsulation of catalase by COS in water solution should carefully be considered due to the

Table 1
Fractions of typical feature of a secondary structure of native catalase and catalase released from $CaCO_3$ crystals (catalase loaded by COS).

Cat	α-helix [%]	α-antiparallel [%]	β-sheet [%]	β-turn [%]	Random coil [%]
native	30.0	9.5	9.7	17.4	35.1
after COS and dialysis	26.5	11.0	10.7	18.3	36.9

high pH of about 10 during the crystal synthesis in water (result of the hydrolysis of $CaCO_3$). This may significantly affect the bioactivity of the encapsulated proteins.

The influence of 0.2 M EDTA on the catalase activity at different pH was also evaluated and no loss of the specific activity was found. Analysis of the catalase activity after catalase loading in $CaCO_3$ crystals by COS followed by the dissolution of the crystals with 0.2 M EDTA reveals that the enzymatic activity significantly drops to approximately 50% at each pH in the range 8–10 (Fig. 8b). The only conclusion one can make is that the catalase activity is significantly affected by its aggregation during the loading into the crystals by COS. It is reported[71] that inter-protein interactions are most probably responsible for the loss of the activity meaning that the protein aggregation during the COS process is partly irreversible in terms of change of the protein secondary structure. However, it does not completely suppress the bioactivity of the loaded protein but reduces it approximately to a half. The loss of activity after COS is likely related to the salt-induced aggregation of enzyme molecules [72].

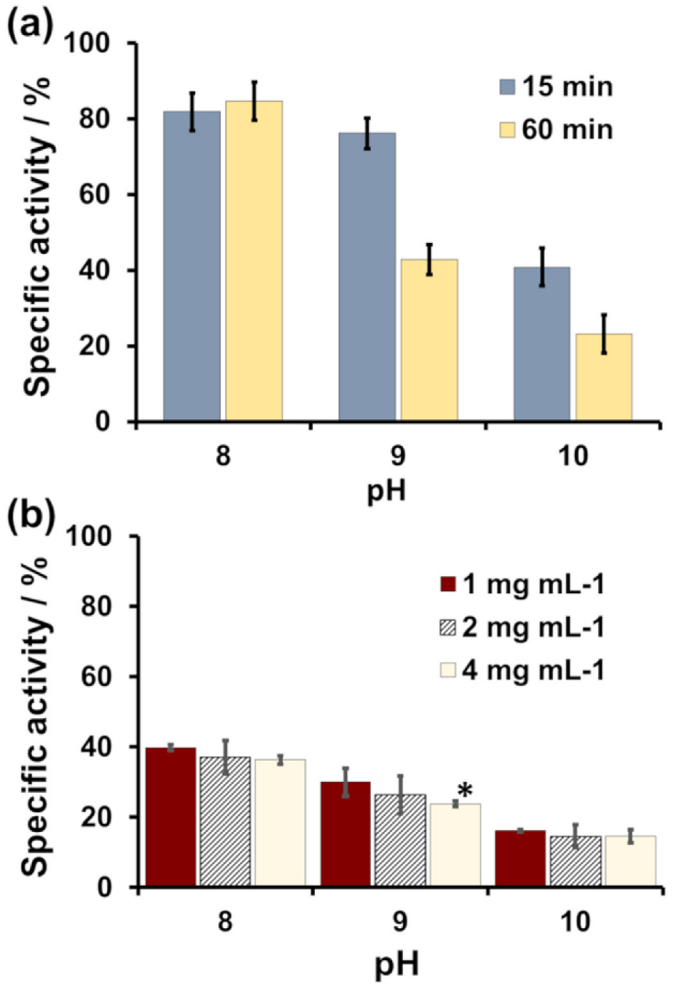

Fig. 8. (a) The influence of pH on the retention of activity of native catalase (1 mg mL^{-1}) after incubation in 0.05 M TRIS buffer for 15 min (grey) or 60 min (yellow) at different pH. (b) The influence of the pH on the specific catalase activity at different initial catalase concentration used for the protein loading into $CaCO_3$ crystals by COS. Catalase loaded into vaterite crystals has been released after dissolution of the crystals by addition of 0.2 M EDTA. Activity of native enzyme in phosphate buffer was taken as 100%. *The difference is statistically significant ($P < 0.01$ versus C_0 of 1 mg mL^{-1} at pH 9).

It is of note that the catalase loaded into the crystals at pH 9.0 by ADS keeps 79 ± 5% of its activity after solubilization of the crystals [59]. Along with that, it should be noted that since the retention of catalase activity strongly depends on time catalase is being exposed to the alkaline solution (Fig. 8a), the main impact into the loss of catalase activity remains to be caused by the long-time exposure in the alkaline pH while the loss of catalase activity caused by the aggregation during the COS is relatively small. For instance, for ADS at pH 9 the loss of catalase activity is ~20% that corresponds to the loss of activity due to exposure into the solution with pH 9 for 15 min (Fig. 8a). At the same time, the catalase exposed into the alkaline solution for 60 min loses ~57% of its activity and COS-associated aggregation leads to the additional loss of only ~13% of catalase activity resulting in the final loss of ~70%. Therefore, for pH 9 the impact of alkaline-induced denaturation of the catalase is approximately 4.4 times higher than the impact of the Ca^{2+}-induced aggregation. The interplay between these two factors - alkaline-induced denaturation and salt-induced aggregation of the catalase during COS - strongly depends on pH (Supporting Information Table S1).

Besides the effect of pH, we have also tested how the protein activity is affected by the content of the protein loaded into the crystals by COS. For this reason, the $CaCO_3$ crystals have been prepared at different concentrations of the loaded catalase (1, 2, and 4 mg mL^{-1}). The retention of the specific catalase activity has been evaluated and one can see that the retained activity is slightly reduced with an increase of the loading concentration at all tested pH values (Fig. 8b). The trend is more pronounced at pH 9 compared to pH 8 and 10. This finding means that at a higher concentration of the loaded protein, the level of catalase aggregation elevates resulting in a more pronounced reduction of the protein activity, presumably due to a larger number of inter-protein contacts in larger aggregates formed at higher initial concentrations of the loaded protein.

4. Conclusion

In this paper, we have investigated the effect of pH on catalase loading into vaterite crystals taking into account both, efficiency of loading and the retention of catalase specific activity. We found that catalase loading capacity does not significantly depend on pH in the range 8–10 for both loading by ADS of COS. This can be explained by a minor impact of electrostatics (van der Waals attractions dominate) because of a low absolute charge of the crystals and a permanent negative but also rather low charge of catalase in the studied pH range. Absolute values of ζ-potentials for either of them are within 15 mV. The activity of catalase was evaluated after dissolution of the crystals in EDTA showing stronger reduction of the activity for COS than for ADS giving of about 30 and 80% of residual activity at loading at pH 9.0, respectively. The loss of the catalase activity is associated with two reasons: i) alkaline-induced

denaturation of the catalase and ii) Ca^{2+}-induced aggregation of the catalase during COS. Notably, while the loading capacity of the crystals is pH-independent, the loss of catalase activity strongly depends on pH. Meanwhile, the loss of catalase activity is not accompanied by the drastic changes in its secondary structure that is almost fully recovered after COS although some reorganization of α-helices has been detected. This indicates a strong inter-protein interaction for the partly reversible process of the protein aggregation. Altogether, these findings indicate that the active encapsulation of proteins by COS should carefully be considered since the preparation pH might have a strong influence on the bioactivity of the encapsulated proteins. Finally, it has to be noted that despite of the significant loss of the catalase activity during COS compared to ADS (about three times difference), the adsorption capacity of the crystals loaded by COS is up to six times higher than that for ADS. This results in the release of nearly two-fold amount of active protein after crystal dissolution for COS versus ADS. In addition, the aggregation during COS results in significant suppression of the catalase release from the crystals. In conclusion, our data suggest an approach for protein encapsulation into vaterite crystals at mild conditions and illustrate the role of preparation pH in the preservation of enzymatic activity of protein-based drug as exemplified by the catalase. We also indicate the pivotal role of non-electrostatic nature of the interaction between the catalase and the crystals which might be the key for the understanding of tremendous capacity that vaterite possesses for this protein (e.g. 170 mg g^{-1} at C_0 4 mg mL^{-1}) and a number of other macromolecules. In spite of the growing number of recent studies which indicate the successful encapsulation of fragile proteins and macromolecules into the $CaCO_3$ crystals, this work serves as a guide for controlled protein-friendly encapsulation.

Data availability

The raw/processed data required to reproduce these findings cannot be shared at this time due to technical or time limitations.

Authorship contribution statement

The manuscript was written through contributions of all authors. All authors have given approval to the final version of the manuscript.

CRediT authorship contribution statement

Natalia A. Feoktistova: Data curation, Investigation, Formal analysis, Methodology, Writing - review & editing. **Anna S. Vikulina:** Data curation, Conceptualization, Formal analysis, Methodology, Project administration, Writing - original draft, Writing - review & editing. **Nadezhda G. Balabushevich:** Data curation, Funding acquisition, Resources, Formal analysis, Methodology, Investigation, Project administration, Supervision, Writing - review & editing. **Andre G. Skirtach:** Conceptualization, Methodology, Investigation, Writing - review & editing. **Dmitry Volodkin:** Conceptualization, Data curation, Funding acquisition, Resources, Formal analysis, Methodology, Project administration, Supervision, Writing - review & editing.

Acknowledgment

The work was performed within the framework of the M.V. Lomonosov Moscow State University state task, part 2 (government grant AAAA-A16-116052010081-5). This work was supported in part by M.V. Lomonosov Moscow State University Program of Development. D.V. acknowledges QR Fund 2018–2019 from Nottingham Trent University. A.V. thanks the Europeans Union's Horizon 2020 research and innovation programme for funding (the Marie-Curie Individual Fellowship LIGHTOPLEX-747245). A.S. acknowledges support of BOF UGent (01IO3618) and Research Foundation - Flanders FWO (G043219). The authors thank Rona Pitschke, Heike Runge, Jacob Ward and Kathryn Kroon for SEM imaging, and Kudryashova Elena for CD discussion.

Appendix A. Supplementary data

Supplementary data to this article can be found online at https://doi.org/10.1016/j.matdes.2019.108223.

References

[1] B. Leader, Q.J. Baca, D.E. Golan, Protein therapeutics: a summary and pharmacological classification, Nat. Rev. Drug Discov. 7 (2008) 21–39.
[2] S. Yang, W. Yuan, T. Jin, Formulating protein therapeutics into particulate forms, Expert Opin. Drug Deliv. 6 (2009) 1123–1133.
[3] M.L. Tan, P.F.M. Choong, C.R. Dass, Recent developments in liposomes, microparticles and nanoparticles for protein and peptide drug delivery, Peptides 31 (2010) 184–193.
[4] A. Muheem, F. Shakeel, M.A. Jahangir, M. Anwar, N. Mallick, G.K. Jain, M.H. Warsi, F.J. Ahmad, A review on the strategies for oral delivery of proteins and peptides and their clinical perspectives, Saudi pharmaceutical journal SPJ the official publication of the Saudi Pharm. J. 24 (2016) 413–428.
[5] J. Cui, Y. Zhao, Y. Feng, T. Lin, C. Zhong, Z. Tan, S. Jia, Encapsulation of spherical cross-linked phenylalanine ammonia lyase aggregates in mesoporous biosilica, J. Agric. Food Chem. 65 (2017) 618–625.
[6] J. Cui, Z. Tan, P. Han, C. Zhong, S. Jia, Enzyme shielding in a large mesoporous hollow silica shell for improved recycling and stability based on $CaCO_3$ microtemplates and biomimetic silicification, J. Agric. Food Chem. 65 (2017) 3883–3890.
[7] D. Luo, M.S. Hasan, S. Shahid, B.N. Khlebtsov, M.J. Cattell, G.B. Sukhorukov, Gold nanorod mediated chlorhexidine microparticle formation and near-infrared light induced release, Langmuir 33 (2017) 7982–7993.
[8] I.Y. Stetciura, A. Yashchenok, A. Masic, E.V. Lyubin, O.A. Inozemtseva, M.G. Drozdova, E.A. Markvichova, B.N. Khlebtsov, A.A. Fedyanin, G.B. Sukhorukov, D.A. Gorin, D. Volodkin, Composite SERS-based satellites navigated by optical tweezers for single cell analysis, Analyst 140 (2015) 4981–4986.
[9] Z. Dong, L. Feng, W. Zhu, X. Sun, M. Gao, H. Zhao, Y. Chao, Z. Liu, CaCO3 nanoparticles as an ultra-sensitive tumor-pH-responsive nanoplatform enabling real-time drug release monitoring and cancer combination therapy, Biomaterials 110 (2016) 60–70.
[10] J.-L. Wu, C.-Q. Wang, R.-X. Zhuo, S.-X. Cheng, Multi-drug delivery system based on alginate/calcium carbonate hybrid nanoparticles for combination chemotherapy, Colloids Surf., B 123 (2014) 498–505.
[11] D.V. Volodkin, S. Schmidt, P. Fernandes, N.I. Larionova, G.B. Sukhorukov, C. Duschl, H. Möhwald, R. von Klitzing, One-step formulation of protein microparticles with tailored properties: hard templating at soft conditions, Adv. Funct. Mater. 22 (2012) 1914–1922.
[12] N.G. Balabushevich, V.A. Izumrudov, N.I. Larionova, Protein microparticles with controlled stability prepared via layer-by-layer adsorption of biopolyelectrolytes, Polym. Sci. Ser. A 54 (2012) 540–551.
[13] J.H.E. Cartwright, A.G. Checa, J.D. Gale, D. Gebauer, C.I. Sainz-Díaz, Calcium carbonate polyamorphism and its role in biomineralization: how many amorphous calcium carbonates are there? Angew. Chem. Int. Ed. 51 (2012) 11960–11970.
[14] B. Ramalapa, O. Crasson, M. Vandevenne, A. Gibaud, E. Garcion, T. Cordonnier, M. Galleni, F. Boury, Protein–polysaccharide complexes for enhanced protein delivery in hyaluronic acid templated calcium carbonate microparticles, J. Mater. Chem. B 5 (2017) 7360–7368.
[15] A. Wang, Y. Yang, X. Zhang, X. Liu, W. Cui, J. Li, Gelatin-assisted synthesis of vaterite nanoparticles with higher surface area and porosity as anticancer drug containers in vitro, ChemPlusChem 81 (2016) 194–201.
[16] B.V. Parakhonskiy, A. Haase, R. Antolini, Sub-micrometer vaterite containers: synthesis, substance loading, and release, Angew. Chem. Int. Ed. 51 (2012) 1195–1197.
[17] F. Baldassarre, C. Allegretti, D. Tessaro, E. Carata, C. Citti, V. Vergaro, C. Nobile, G. Cannazza, P. D'Arrigo, A. Mele, L. Dini, G. Ciccarella, Biocatalytic synthesis of phospholipids and their application as coating agents for $CaCO_3$ nano-crystals: characterization and intracellular localization analysis, ChemistrySelect 1 (2016) 6507–6514.
[18] E.P. Mironov, I.V. Marchenko, V.V. Artemov, T.V. Bukreeva, A study of the interaction between polyelectrolyte-coated nanostructured $CaCO_3$ particles and a stearic acid monolayer spread at the water/air interface, Colloid J. 79 (2017) 360–367.
[19] D.B. Trushina, T.V. Bukreeva, M.N. Antipina, Size-controlled synthesis of vaterite calcium carbonate by the mixing method: aiming for nanosized

particles, Cryst. Growth Des. 16 (2016) 1311–1319.
[20] N.G.M. Palmqvist, J.-M. Nedelec, G.A. Seisenbaeva, V.G. Kessler, Controlling nucleation and growth of nano-$CaCO_3$ via CO_2 sequestration by a calcium alkoxide solution to produce nanocomposites for drug delivery applications, Acta Biomater. 57 (2017) 426–434.
[21] A. Achour, A. Arman, M. Islam, A.A. Zavarian, A. Basim Al-Zubaidi, J. Szade, Synthesis and characterization of porous $CaCO_3$ micro/nano-particles, Eur. Phys. J. Plus 132 (2017) 14473.
[22] N. Feoktistova, J. Rose, V.Z. Prokopović, A.S. Vikulina, A. Skirtach, D. Volodkin, Controlling the vaterite $CaCO_3$ crystal pores. Design of tailor-made polymer based microcapsules by hard templating, Langmuir 32 (2016) 4229–4238.
[23] L.N. Hassani, F. Hindré, T. Beuvier, B. Calvignac, N. Lautram, A. Gibaud, F. Boury, Lysozyme encapsulation into nanostructured $CaCO_3$ microparticles using a supercritical CO2 process and comparison with the normal route, J. Mater. Chem. B 1 (2013) 4011.
[24] A. Sergeeva, R. Sergeev, E. Lengert, A. Zakharevich, B. Parakhonskiy, D. Gorin, S. Sergeev, D. Volodkin, Composite magnetite and protein containing $CaCO_3$ crystals. External manipulation and vaterite → calcite recrystallization-mediated release performance, ACS Appl. Mater. Interfaces 7 (2015) 21315–21325.
[25] B.V. Parakhonskiy, A.M. Yashchenok, S. Donatan, D.V. Volodkin, F. Tessarolo, R. Antolini, H. Möhwald, A.G. Skirtach, Macromolecule loading into spherical, elliptical, star-like and cubic calcium carbonate carriers, ChemPhysChem 15 (2014) 2817–2822.
[26] S. Donatan, A. Yashchenok, N. Khan, B. Parakhonskiy, M. Cocquyt, B.-E. Pinchasik, D. Khalenkow, H. Möhwald, M. Konrad, A. Skirtach, Loading capacity versus enzyme activity in anisotropic and spherical calcium carbonate microparticles, ACS Appl. Mater. Interfaces 8 (2016) 14284–14292.
[27] A.A. Antipov, G.B. Sukhorukov, S. Leporatti, I.L. Radtchenko, E. Donath, H. Möhwald, Polyelectrolyte multilayer capsule permeability control, Colloids Surf., A 198–200 (2002) 535–541.
[28] K. Ariga, M. McShane, Y.M. Lvov, Q. Ji, J.P. Hill, Layer-by-layer assembly for drug delivery and related applications, Expert Opin, Drug Deliv. 8 (2011) 633–644.
[29] K. Ariga, Y.M. Lvov, K. Kawakami, Q. Ji, J.P. Hill, Layer-by-layer self-assembled shells for drug delivery, Adv. Drug Deliv. Rev. 63 (2011) 762–771.
[30] M. Delcea, H. Möhwald, A.G. Skirtach, Stimuli-responsive LbL capsules and nanoshells for drug delivery, Adv. Drug Deliv. Rev. 63 (2011) 730–747.
[31] J. Cui, Y. Zhao, Z. Tan, C. Zhong, P. Han, S. Jia, Mesoporous phenylalanine ammonia lyase microspheres with improved stability through calcium carbonate templating, Int. J. Biol. Macromol. 98 (2017) 887–896.
[32] S. Schmidt, M. Behra, K. Uhlig, N. Madaboosi, L. Hartmann, C. Duschl, D. Volodkin, Mesoporous protein particles through colloidal $CaCO_3$ templates, Adv. Funct. Mater. 23 (2013) 116–123.
[33] P.K. Harimech, R. Hartmann, J. Rejman, P. del Pino, P. Rivera-Gil, W.J. Parak, Encapsulated enzymes with integrated fluorescence-control of enzymatic activity, J. Mater. Chem. B 3 (2015) 2801–2807.
[34] Z. Ergul Yilmaz, T. Cordonnier, A. Debuigne, B. Calvignac, C. Jerome, F. Boury, Protein encapsulation and release from PEO-b-polyphosphoester templated calcium carbonate particles, Int. J. Pharm. (Amsterdam, Neth.) 513 (2016) 130–137.
[35] P.V. Binevski, N.G. Balabushevich, V.I. Uvarova, A.S. Vikulina, D. Volodkin, Biofriendly encapsulation of superoxide dismutase into vaterite $CaCO_3$ crystals. Enzyme activity, release mechanism, and perspectives for ophthalmology, Colloids Surf., B 181 (2019) 437–449.
[36] N.G. Balabushevich, E.A. Kovalenko, I.M. Le-Deygen, L.Y. Filatova, D. Volodkin, A.S. Vikulina, Hybrid $CaCO_3$-mucin crystals: effective approach for loading and controlled release of cationic drugs, Mater. Des. 182 (2019) 108020.
[37] N.G. Balabushevich, E.A. Kovalenko, E.V. Mikhalchik, L.Y. Filatova, D. Volodkin, A.S. Vikulina, Mucin adsorption on vaterite $CaCO_3$ microcrystals for the prediction of mucoadhesive properties, J. Colloid Interface Sci. 545 (2019) 330–339.
[38] N.A.N. Hanafy, M.L. de Giorgi, C. Nobile, M. Cascione, R. Rinaldi, S. Leporatti, $CaCO_3$ rods as chitosan-polygalacturonic acid carriers for bromopyruvic acid delivery, Sci. Adv. Mater. 8 (2016) 514–523.
[39] X. Liu, S. She, W. Tong, C. Gao, Preparation of elastic polyurethane microcapsules using $CaCO_3$ microparticles as templates for hydrophobic substances loading, RSC Adv. 5 (2015) 5775–5780.
[40] Y. Jin, R. Yendluri, B. Chen, J. Wang, Y. Lvov, Composite microparticles of halloysite clay nanotubes bound by calcium carbonate, J. Colloid Interface Sci. 466 (2016) 254–260.
[41] M. Behra, N. Azzouz, S. Schmidt, D.V. Volodkin, S. Mosca, M. Chanana, P.H. Seeberger, L. Hartmann, Magnetic porous sugar-functionalized PEG microgels for efficient isolation and removal of bacteria from solution, Biomacromolecules 14 (2013) 1927–1935.
[42] M. Behra, S. Schmidt, J. Hartmann, D.V. Volodkin, L. Hartmann, Synthesis of porous PEG microgels using $CaCO_3$ microspheres as hard templates, Macromol. Rapid Commun. 33 (2012) 1049–1054.
[43] N. Feoktistova, G. Stoychev, N. Puretskiy, L. Ionov, D. Volodkin, Porous thermoresponsive pNIPAM microgels, Eur. Polym. J. 68 (2015) 650–656.
[44] J. Jia, Q. Liu, T. Yang, L. Wang, G. Ma, Facile fabrication of varisized calcium carbonate microspheres as vaccine adjuvants, J. Mater. Chem. B 5 (2017) 1611–1623.
[45] S. Schmidt, K. Uhlig, C. Duschl, D. Volodkin, Stability and cell uptake of calcium carbonate templated insulin microparticles, Acta Biomater. 10 (2014) 1423–1430.
[46] D. Liu, G. Jiang, W. Yu, L. Li, Z. Tong, X. Kong, J. Yao, Oral delivery of insulin using $CaCO_3$-based composite nanocarriers with hyaluronic acid coatings, Mater. Lett. 188 (2017) 263–266.
[47] T.N. Borodina, D.B. Trushina, I.V. Marchenko, T.V. Bukreeva, Calcium carbonate-based mucoadhesive microcontainers for intranasal delivery of drugs bypassing the blood–brain barrier, BioNanoSci 6 (2016) 261–268.
[48] M.A. Vantsyan, A.A. Kochetkov, I.V. Marchenko, Y.I. Kiryukhin, B.V. Nabatov, V.V. Artemov, T.V. Bukreeva, Nanostructured calcium carbonate particles as fluorophore carriers, Crystallogr. Rep. 60 (2015) 951–958.
[49] Q. Dong, J. Li, L. Cui, H. Jian, A. Wang, S. Bai, Using porous $CaCO_3$/hyaluronic acid nanocages to accommodate hydrophobic photosensitizer in aqueous media for photodynamic therapy, Colloid Surf. A. 516 (2017) 190–198.
[50] N. Balabushevich, E. Sholina, E. Mikhalchik, L. Filatova, A. Vikulina, D. Volodkin, Self-Assembled mucin-containing microcarriers via hard templating on $CaCO_3$ crystals, Micromachines 9 (2018) 307.
[51] P.W.J. Morrison, V.V. Khutoryanskiy, Advances in ophthalmic drug delivery, Ther. Deliv. 5 (2014) 1297–1315.
[52] O.M. Kolawole, W.M. Lau, H. Mostafid, V.V. Khutoryanskiy, Advances in intravesical drug delivery systems to treat bladder cancer, Int. J. Pharm. (Amsterdam, Neth.) 532 (2017) 105–117.
[53] A.S. Sergeeva, D.A. Gorin, D.V. Volodkin, In-situ assembly of Ca-alginate gels with controlled pore loading/release capability, Langmuir 31 (2015) 10813–10821.
[54] A. Sergeeva, N. Feoktistova, V. Prokopovic, D. Gorin, D. Volodkin, Design of porous alginate hydrogels by sacrificial $CaCO_3$ templates: pore formation mechanism, Adv. Mater. Interfaces 2 (2015) 1500386.
[55] T. Paulraj, N. Feoktistova, N. Velk, K. Uhlig, C. Duschl, D. Volodkin, Microporous polymeric 3D scaffolds templated by the layer-by-layer self-assembly, Macromol. Rapid Commun. 35 (2014) 1408–1413.
[56] N.E. Markina, A.V. Markin, A.M. Zakharevich, I.Y. Goryacheva, Calcium carbonate microparticles with embedded silver and magnetite nanoparticles as new SERS-active sorbent for solid phase extraction, Microchim Acta 184 (2017) 3937–3944.
[57] M. Abebe, N. Hedin, Z. Bacsik, Spherical and porous particles of calcium carbonate synthesized with food friendly polymer additives, Cryst. Growth Des. 15 (2015) 3609–3616.
[58] D.B. Trushina, T.V. Bukreeva, M.V. Kovalchuk, M.N. Antipina, $CaCO_3$ vaterite microparticles for biomedical and personal care applications, Mater. Sci. Eng. C 45 (2014) 644–658.
[59] N.G. Balabushevich, A.V. Lopez de Guerenu, N.A. Feoktistova, D. Volodkin, Protein loading into porous $CaCO_3$ microspheres: adsorption equilibrium and bioactivity retention, Phys. Chem. Chem. Phys. 17 (2015) 2523–2530.
[60] A.S. Vikulina, N.A. Feoktistova, N.G. Balabushevich, A.G. Skirtach, D. Volodkin, The mechanism of catalase loading into porous vaterite $CaCO_3$ crystals by co-synthesis, Phys. Chem. Chem. Phys. 20 (2018) 8822–8831.
[61] A.G. Grigoras, Catalase immobilization—a review, Biochem. Eng. J. 117 (2017) 1–20.
[62] N.G. Balabushevich, E.P. Zimina, N.I. Larionova, Encapsulation of catalase in polyelectrolyte microspheres composed of melamine formaldehyde, dextran sulfate, and protamine, Biochemistry, Biokhimiia 69 (2004) 763–769.
[63] N.G. Balabushevich, A.V. Lopez de Guerenu, N.A. Feoktistova, A.G. Skirtach, D. Volodkin, Protein-containing multilayer capsules by templating on mesoporous $CaCO_3$ particles: POST- and PRE-loading approaches, Macromol. Biosci. 16 (2016) 95–105.
[64] K.Y. Chong, C.H. Chia, S. Zakaria, M.S. Sajab, Vaterite calcium carbonate for the adsorption of Congo red from aqueous solutions, J. Environ. Chem. Eng. 2 (2014) 2156–2161.
[65] L. Bergström, Hamaker constants of inorganic materials, Adv. Colloid Interf. Sci 70 (1997) 125–169.
[66] S. Beretta, G. Chirico, G. Baldini, Short-range interactions of globular proteins at high ionic strengths, Macromolecules 33 (2000) 8663–8670.
[67] N.I. Lebovka, Aggregation of charged colloidal particles, in: M. Müller (Ed.), Polyelectrolyte Complexes in the Dispersed and Solid State I: Principles and Theory, Springer Berlin Heidelberg, Berlin, Heidelberg, 2014, pp. 57–96.
[68] A.I. Petrov, D.V. Volodkin, G.B. Sukhorukov, Protein-calcium carbonate coprecipitation: a tool for protein encapsulation, Biotech. Prog. 21 (2005) 918–925.
[69] D.V. Volodkin, N.I. Larionova, G.B. Sukhorukov, Protein encapsulation via porous $CaCO_3$ microparticles templating, Biomacromolecules 5 (2004) 1962–1972.
[70] D.V. Volodkin, N.G. Balabushevitch, G.B. Sukhorukov, N.I. Larionova, Model system for controlled protein release: pH-sensitive polyelectrolyte microparticles, STP Pharma Sci. 13 (2003) 163–170.
[71] C.J. Reed, S. Bushnell, C. Evilia, Circular dichroism and fluorescence spectroscopy of cysteinyl-tRNA synthetase from Halobacterium salinarum ssp. NRC-1 demonstrates that group I cations are particularly effective in providing structure and stability to this halophilic protein, PLoS One 9 (2014), e89452.
[72] S. Prajapati, V. Bhakuni, K.R. Babu, S.K. Jain, Alkaline unfolding and salt-induced folding of bovine liver catalase at high pH, Eur. J. Biochem. 255 (1998) 178–184.